Chiang Mai J. Sci. 2016; 43(1) : 183-194
http://epg.science.cmu.ac.th/ejournal/
Contributed Paper

# Validating Adsorptive Capacity of Areca Husk Carbon onto Methylene Blue with ANOVA Modeling

**Arumugam Basker*[a], Syed Shabudeen [b], Appavoo Ponnuraju Shekhar [c] and Savarimuthu Daniel [b]**

[a] Department of Chemistry, Kalaignar Karunanidhi Institute of Technology, Coimbatore-641402, Tamil Nadu, India.

[b] Department of Chemistry, Kumaraguru College of Technology, Coimbatore-641049, Tamil Nadu, India.

[c] Department of Chemistry, Chikkanna Govt Arts College, Tirupur-641602, Tamil Nadu, India.

*Author for correspondence; e-mail: baskerchemistry@gmail.com

Received: 11 December 2013
Accepted: 7 October 2014

## ABSTRACT

ANOVA, chemical kinetics parameters are effectively to optimize the absorptive capacity of an indigenously prepared adsorbent. In this study, the ability of areca husk carbon to adsorb methylene blue (MB) dye from aqueous solution was investigated. Batch experiments were carried out for the adsorption of dye molecules onto AHC at room temperature. The influences of various factors such as particle size, adsorbent dosage, initial dye concentration, contact time, pH and temperature on the adsorption capacity were investigated and optimal experimental conditions were ascertained. Adsorption data were modeled using Langmuir, Freundlich and Temkin adsorption isotherms. Adsorption kinetics were verified by pseudo-first order, pseudo-second order and intraparticle diffusion models. The kinetic adsorption data fitted with the pseudo-first order kinetic model and intra-particle diffusion model. Thermodynamic parameters have been evaluated. The structural and morphology of the activated carbon were characterized by FTIR and SEM studies. Main and interaction effects were analysed by analysis of variance (ANOVA), F-test and p-values are used to define most important process variables affecting the dye adsorption. The results indicated that AHC could be employed as a low cost adsorbent in wastewater treatment for the removal of MB.

**Keywords:** adsorption, areca husk, methylene blue

## 1. INTRODUCTION

Many manufacturing industries such as paper, plastics, cosmetics, textile and food use dyes for colouring their products. The discharge of effluents from these industries contain large amount of dyes, which not only damage the aesthetic nature of receiving water bodies, but also creates toxicity to aquatic life. Methylene Blue has wide applications which include colouring paper, dyeing cottons, wools, silk, leather and coating for paper stock. Although methylene blue is not so hazardous, but it can cause some harmful effects, such as nausea, stomach upset, diarrhoea, vomiting or bladder irritation may occur. It also causes the undesired colour to urine, stools and possibly skin to turn green-blue in colour, high fever, abdominal pain, headache, chest pain, dizziness, profuse sweating, heart beat increase, shock, cyanosis,

jaundice, quadriplegia, and tissue necrosis in humans[1]. Therefore, the treatment of effluents containing such dyes is of great interest due to this harmful impacts.

There are several works of low cost non-conventional adsorbents has been carried out so far. Adsorbents used include agricultural solid wastes such as Walnut shell, Almond shell, Hazelnut shell and Apricot stones[2], Sludge ash[3], Fine grinded wheat straw and Coarse grinded wheat straw[4], Caulerpa racemosa[5], Fly ash treated with $HNO_3$[6], Kaolin [7], Modified bamboo[8], Indian rosewood sawdust[9], Wheat shells[10], Natural Tripoli[11], Picea abies[12], Albizia seed pods[13], Cereal chaff, Jute processing waste and Yellow fashion fruit waste[14], Salsola vermiculata leaves[15], Tea waste[16], Pitch-pine saw dust Cherry saw dust and Oak saw dust[17], Green grass[18], Daucus carota[19], Mansonia wood sawdust[20], Parthenium[21], Rice husk[22], Olive pomice[23]. The aim of the present study is to prepare and characterize the quality and evaluate its efficiency of AHC as an adsorbent for the removal of Methylene blue. After considering the efficiency of colour removal, the study was extended for other adsorbate and such study has not been attempted earlier. The adsorption study was carried out systematically involving various parameters such as time, initial dye concentration, particle size, adsorbent dosage, particle size, pH and temperature. The data generated over this study have been tabulated and discussed. The cost of this activated carbon is estimasted and it is 10 times less than that of commercially available activated carbon.

## 2. MATERIALS AND METHODS

### 2.1 Preparation of Activated Carbon

One part by weight of each powdered raw material was chemically activated by treating with two parts by weight of concentrated sulphuric acid with constant stirring and was kept for 24 hours in a hot air oven at 75°C, the carbonized material was washed well with plenty of water several times to remove excess acid, surface adhered particles, water soluble materials and dried at 200°C in a hot air oven for 24 hours. The adsorbent thus obtained was grounded well and kept in a air tight containers for further use.

### 2.2 Analysis of Methylene Blue

MB supplied by Sigma–Aldrich (M) Sdn Bhd, Malaysia was used as an adsorbate and was not purified prior to use. Distilled water was employed in preparing all the solutions and reagents. MB has a molecular weight of 374 g $mol^{-1}$, which corresponds to the methylene blue hydrochloride with three groups of water. The concentration of MB in the supernatant solution after and before adsorption was determined using a double beam UV spectrophotometer (Shimadzu, Japan) at 665 nm. It was found that the supernatant from the activated carbon did not exhibit any absorbance at this wavelength and also that the calibration curve was very reproducible and linear over the concentration range used in this work.

### 2.3 Batch Equilibrium Studies

MB solutions were prepared with distilled water. Batch experiments were carried in a glass beaker by shaking a fixed mass AHC (150 mg) with 100ml diluted solution (20-100 mg $L^{-1}$). After agitation the solution is centrifuged at 1200 rpm. Then the dye concentration in the supernatant solution was analysed by using a spectrophotometer by monitoring the absorbance changes at a wavelength of maximum absorbance (665nm) in these sorption experiments, the solution pH was used without adjusting pH 6.3. Each experiment was carried out in duplicate and the average results are presented. Calibration curves were obtained with standard MB solution by using distilled water as a blank. Mass capacity of adsorption

$q_e$ is calculated from the difference between the initial and final MB. concentration.

$$q_e = \frac{(C_o - C_e)}{W} \quad (1)$$

Where $C_0$ and $C_e$ (mg $L^{-1}$) are the liquid-phase concentrations of dye at initial and equilibrium respectively. V is the volume of the solution (l), and W is the mass of dry adsorbent used (g).

## 3. RESULTS AND DISCUSSION

### 3.1 Characterization of AHC

The fixed carbon content of the adsorbent is nearly 80% this results in low ash content and from the analysis. From the solubility studies, the presence of impurities can be detected and these impurities will affect the quality of the treated water. It was observed that the AHC contains only the permitted level of impurities. The incorporation of acid in the carbon structure makes it acidic in nature (pH 6.3) with very little ion exchange capacity because it was activated by an acid treatment process. The characterization of activated carbon shows that the iron content was very minimal and the leaching problem of iron into treated water was satisfactorily ruled out. The phenol adsorption capacity and decolourizing power were 11.2 and 22.6 mg $L^{-1}$, respectively, which indicates that the carbon prepared by acid activation method has the adsorption capacity and it can be considered for the adsorption of organic dyes.

### 3.2 Surface Characterization

The FT-IR spectrum of MB on AHC before and after adsorption was detected in the range of 4000 to 400 $cm^{-1}$ and is presented in Figure 1. The band observed at 3425.6$cm^{-1}$ was assigned to a $\nu$(O-H) stretching vibration. The absorption band at 2854.7 and 2924.1$cm^{-1}$ can be attributed to the stretching vibrations of $\nu$(C-H) bonds in alkane and alkyl groups where carbon is bonded with hydrogen bonds. Adsorption bands at 2337.7 and 2376.3$cm^{-1}$ were corresponds to $\nu$(N-H) stretching. The band at 1573.9$cm^{-1}$ shows the asymmetric $\nu$(-COO-) stretching. The band at 1450.5$cm^{-1}$ may be attributed to the aromatic $\nu$(C=C) stretching

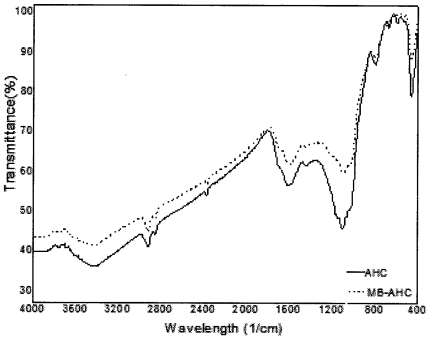


**Figure 1.** FTIR spectra of fresh and MB loaded AHC.

**Table 1.** Characteristics of areca husk carbon.

| S.No. | Parameters | Obtained Results | S.No. | Parameters | Obtained Results |
|---|---|---|---|---|---|
| 1 | PH 1% Solution | 6.3 | 11 | Moisture content (%) | 2.4 |
| 2 | Carbon (%) | 79.76 | 12 | Ash content (%) | 1.8 |
| 3 | Oxygen (%) | 15.85 | 13 | Decolourizing power (mg/g) | 22.6 |
| 4 | Sodium (%) | 0.35 | 14 | Ion-exchange capacity (milli eq./g) | 0.0415 |
| 5 | Aluminium (%) | 0.55 | 15 | Surface area ($m^2$/g) | 285 |
| 6 | Silicon (%) | 2.84 | 16 | Bulk Density (g/L) | 0.42 |
| 7 | Sulphur (%) | 0.21 | 17 | Pore size (nm) | 5.43 |
| 8 | Chloride (%) | 0.11 | 18 | Water soluble matter (%) | 2 |
| 9 | Potassium (%) | 0.09 | 19 | Acid soluble matter (%) | 7 |
| 10 | Calcium (%) | 0.25 | 20 | Phenol number | 11.2 |

vibration. At 1111.0cm$^{-1}$, the band is highly intense $\nu$(C-O) and is related to the $\nu$(C-O) stretching vibration of the bonds in ester, ether, or phenol groups. The band corresponding to 802.4cm$^{-1}$ in the fingerprint area indicates a mono substituted aromatic structure. The weak absorption band at 678.9cm$^{-1}$ corresponds to the $\nu$(O-H) vibration in the benzene ring. The band at 462.9 and 594.1cm$^{-1}$ which were associated with in plane and out-of-plane aromatic ring deformation vibrations which are quite common for activated carbon. Some of the peak were disappeared due to the absorption of MB on AHC. The absorption bands at 1381cm$^{-1}$ may be assigned to $\nu$(N-O) stretching, indicating that MB was adsorbed on the surface of AHC.

### 3.3 SEM Images

It is widely used to study the morphological features and surface characteristics of the adsorbent materials. Typical SEM photographs are shown in Figure 2. It reveals that the AHC has a rough surface with more porous and caves like structure. The SEM Figure 3 shows the morphology of the loaded adsorbent, the surface of the adsorbent due to adsorption of the MB dye molecules. A close scrutiny of SEM micrograph further indicates with the density difference before and after adsorption of dyes onto AHC which confirming the uptake of dye molecules in waste water.

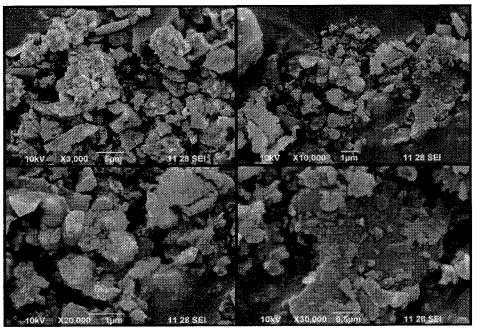

**Figure 2.** SEM image of Fresh AHC.

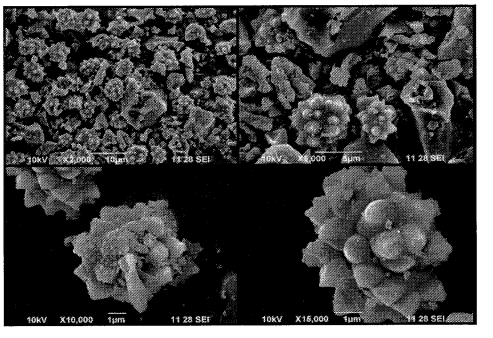

**Figure 3.** SEM image of MB loaded AHC.

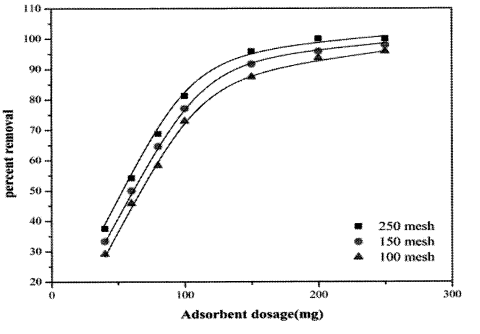


**Figure 4.** Influence of adsorbent Dosage and particle size on the removal of MB dye onto AHC.

### 3.4 Influence of Adsorbent Dosage

In order to study the effect of adsorbent dosage on the adsorption of MB, a series of adsorption experiments was carried out with different adsorbent dosages an initial dye concentration of 10 mg L$^{-1}$. Figure 4 shows the effect of adsorbent dose on the removal of MB. Along with the increase of adsorbent dosage from 40-250 mg L$^{-1}$, the percentage of dye adsorbed increased. Above 150 mg of adsorbent dose the equilibrium of the dye was reached and the removal ratios of dyes held almost no variations, so the AHC of 150mg was chosen for subsequent experiments.

### 3.5 Influence of Particle Size

The breaking up of large particles into smaller ones sometimes open tiny cracks and sealed channels on the particle size, which might then become available for adsorption. The

adsorption of smaller particles is higher than larger particles. This is due to larger surface area associated with smaller particles. Experiments were carried out at the appropriate equilibrium time limits to assess the variations on the amount of dyes adsorbed on the adsorbent of different particle sizes like 250, 150, 100 BSS mesh numbers were selected the initial dye concentration being 10mg/100ml. From the experimental investigations, a set of graphs were obtained by plotting % Removal against adsorbent dosages were shown in Figure 4. As the particle of size 250 BSS mesh exhibit maximum adsorption capacity, all further detailed studies were carried out with this particle size only.

### 3.6 Influence of Contact Time

The effect of contact time for the removal of dye was shown in Figure5. It is clear that the extent of adsorption is rapid in the initial stages and becomes slow in later stages till saturation is allowed. The final dye concentration did not vary significantly after 2 hours from the initial stage of adsorption process. This shows that equilibrium can be assumed to be achieved after 2 hours of contact time and was found to be sufficient time to acquire the equilibrium. It is basically due to saturation of the active site which does not allow further adsorption. The adsorption rate was found to decrease with increase in time.

### 3.7 Influence of Initial Dye Concentration

The study of initial dye concentration was studied by varying the dye concentration from 5 to 20 mg $L^{-1}$ leads to a decrease in the percentage of the MB removal respectively. The rapid adsorption takes place in the first 30 min. Then the adsorption rate was decreased gradually and the adsorption reached the equilibrium state. This is because of low adsorbate/adsorbent ratios, there are a number of sorption sites in the AHC but as the ratio

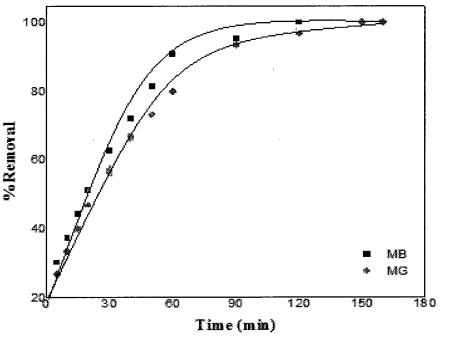


**Figure 5.** Influence of contact time on the removal of MB dye onto AHC.

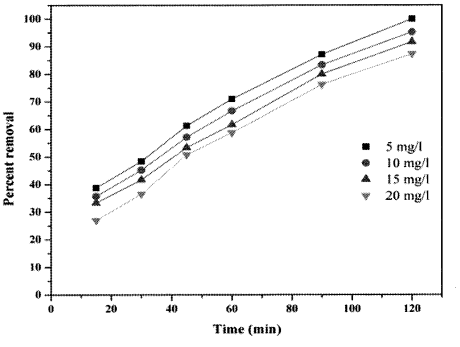


**Figure 6.** Influence of Initial dye concentration on the removal of MB dye onto AHC.

increases the adsorption sites are saturated, resulting to decrease in the sorption efficiency.

### 3.8 Influence of pH

As, the pH of the dye solution plays an important role in the whole adsorption process. As shown in Figure 7 a consistent increase in the dye removal of the AHC was noticed as the pH increased from 2-6, after 6 the adsorption amount was only slightly affected by pH. The percent removal of dye MB found to be 93.7-100. As pH of the system decreased, the number of negatively charged adsorbent sites decreased and the number of positively charged surface sites increased, which did not favour the adsorption of positively charged dye cations due to electrostatic repulsion. In addition, lower adsorption of MB at acidic pH might be due to the presence of excess $H^+$ ions

competing with dye cations for the available adsorption sites.

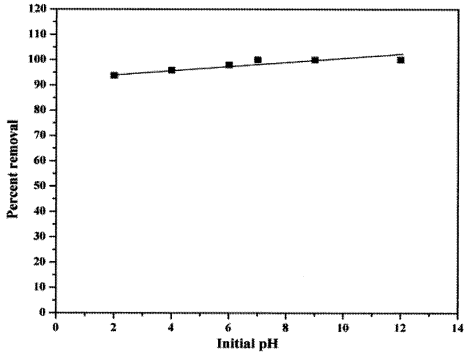


**Figure 7.** Influence of pH on the removal of MB dye onto AHC.

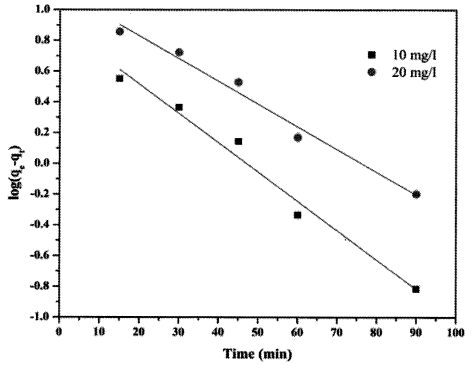


**Figure 8.**Pseudo first order kinetics for the adsorption of MB dye onto AHC.

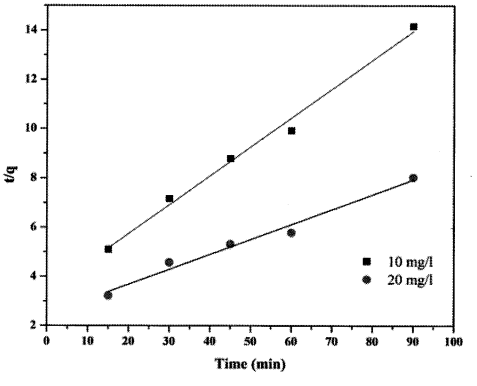


**Figure 9.** Pseudo second order kinetics for the adsorption of MB dye onto AHC.

### 3.9 Adsorption Kinetics

**Pseudo first order kinetic model**

Lagergren proposed a pseudo-first order kinetic model as below [24]. The integrated form of the model is:

$$\log(q_e - q_t) = \log q_e - \frac{k_1}{2.303} t \qquad (2)$$

Where $k_1$ ($min^{-1}$) is the rate constant of the pseudo-first order adsorption and $q_t$ is the adsorption capacity at time't' ($mg\ g^{-1}$) .The rate parameters $k_1$ and $q_e$ can be directly obtained from the intercept and slope of the plot of $\log(q_e - q_t)$ $V_s$ t. The correlation values of $R^2$ were 0.97 and 0.98 for 10 mg $L^{-1}$ and 20 mg $L^{-1}$ respectively. The equilibrium adsorption capacities were 6.51 and 11.35 mg $g^{-1}$respectively. The calculated equilibrium adsorption capacities were 7.89 and 13.34 mg $g^{-1}$. The calculated and experimental results revealed that, the pseudo-first order model provided a better approximation to the experimental kinetic data than the pseudo-second order model for adsorption of MB from aqueous solution. The rate constant and other results obtained graphically were presented in Table2.

**Pseudo-second-order kinetic model**

Pseudo-second-order kinetic model [25] is given as:

$$\frac{t}{q_t} = \frac{1}{k_2 q_e^2} + \frac{t}{q_e} \qquad (3)$$

Where $k_2$ [g $mg^{-1}$ $min^{-1}$] is the rate constant of the pseudo-second order adsorption and $q_t$ is the adsorption capacity at time't' ($mg\ g^{-1}$). The plot of t/q versus t of Equation.5 should give a linear relationship, from which $q_{eq}$ and $k_2$ can be determined from the slope and intercept of the plot are listed in the Table 2.

The correlation values are close to the unity. The rate constant $k_2$ were 0.12 and 0.06 g $mg^{-1}$ $min^{-1}$ for 10 mg $L^{-1}$ and 20 mg $L^{-1}$ respectively. In addition to the $q_e$ calculated values and the experimental values $q_e$ are not similar showing that the adsorption kinetics of

**Table 2.** Adsorption kinetics and isotherm parameters for the adsorption of MB dye onto AHC.

| Kinetic models | | | Isotherm models | |
|---|---|---|---|---|
| Pseudo- first order | Initial Concentration | | Langmuir Isotherm | Model coefficient |
| | 10mg $L^{-1}$ | 20 mg $L^{-1}$ | | |
| $q_e$ (mg $g^{-1}$) | 6.51 | 11.85 | $q_0$(mg $g^{-1}$) | 46.32 |
| $q_{calc}$ (mg $g^{-1}$) | 7.89 | 13.34 | $K_L$(L $mg^{-1}$) | 0.34 |
| $k_1$($min^{-1}$) | -0.019 | -0.015 | $R^2$ | 0.99 |
| $R^2$ | 0.97 | 0.98 | $R_L$ | 0.033 |
| Pseudo-second order | | | Freundlich Isotherm | |
| $q_{calc}$(mg $g^{-1}$) | 3.40 | 2.47 | $k_f$ (mg g-1) | 13.18 |
| $k_2$ (g $mg^{-1}min^{-1}$) | 0.12 | 0.06 | n | 2.55 |
| $R^2$ | 0.98 | 0.98 | $R^2$ | 0.98 |
| Intra-particle diffusion | | | Temkin Isotherm | |
| $k_{int}$ (mg $g^{-1}$ $min^{-0.5}$) | 0.513 | 1.050 | A | 2.99 |
| C | 1.40 | 1.06 | b | 10.26 |
| $R^2$ | 0.90 | 0.94 | B | 243.09 |
| | | | $R^2$ | 0.99 |

the entire process did not follow the pseudo second order model. and follows the pseudo first order model provided a good correlation for the adsorption of MB on AHC.

### Intra-particle diffusion model

In order to understand the diffusion mechanism, kinetic data was further analysed using the intra-particle diffusion model based on the theory proposed by Weber and Morris [26] is given as:

$$q_t = K_{int}t^{0.5} + C \quad (4)$$

Where $q_t$ is the amount of AHC adsorbed (mg $g^{-1}$) $k_{int}$,the intra-particle diffusion rate constant(mg $g^{-1}$ $min^{0.5}$) and C is the intercept is listed in Table 2. $k_{int}$ was determined from the slope of the plot of $q_t$ versus $t^{0.5}$ (figure 10).

The calculated value of $k_{int}$ is 0.513 mg $g^{-1}$ $min^{0.5}$ and C is 1.40. The correlation coefficient ($R^2$) values of 0.90 and 0.94 for the AHC. The high $R^2$ value indicates that intra-particle diffusion might play a significant role in the initial stage of the adsorption. The value of intercept gives an idea about the thickness of the boundary layer. The double nature of the plot may be explained by the fact that the initial portion is the boundary layer diffusion effect while the final linear portion is the result of intra particle diffusion

### 3.10 Isotherm Study

### Langmuir isotherm

The linear transformation of the Langmuir equation [27] is given by

$$\frac{1}{q_e} = \frac{1}{q_0 b C_e} + \frac{1}{q_0} \quad (5)$$

Where $q_o$ is the maximum amount of adsorbate per unit mass of adsorbent form a complete monolayer on the surface (adsorption capacity), $C_e$ denotes equilibrium adsorption concentration

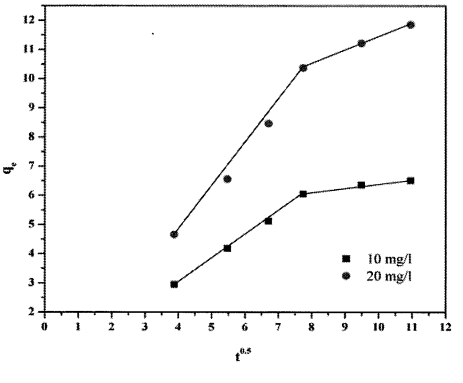


**Figure 10.** Intra particle diffusion plots for the adsorption of MB dye onto AHC.

in solution, $q_e$ is the amount adsorbed per unit mass of adsorbent and b is the binding energy constant. A plot of $1/C_e$ versus $1/q_e$ is graphically represented in Figure11. The values of $Q_0$ and b were calculated from the intercept and slope respectively and the results are presented in Table 2. A further analysis of the Langmuir equation can be made on the basis of a dimensionless equilibrium parameter, $R_L$ also known as the separation factor that is given by the following equation.

$$\mathbf{R_L = \frac{1}{(1 + b\,C_0)}} \quad (6)$$

The data related to the equilibrium obeyed well with the Langmuir models. The maximum adsorption capacity of adsorption of MB by Langmuir isotherm was 46.3 mg $g^{-1}$. The value of $R_L$ was 0.033 which indicates the favour able adsorption i.e. formation of monolayer of MB on the surface of AHC.

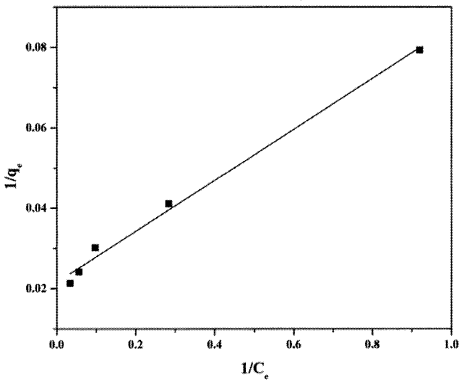


**Figure 11.** Langmuir adsorption isotherm for the adsorption of MB dye onto AHC.

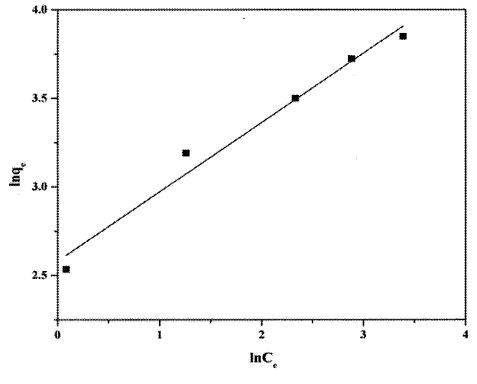


**Figure 12.** Freundlich adsorption isotherms for the adsorption of MB dye onto AHC.

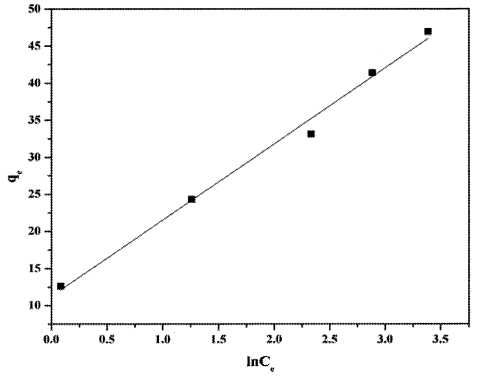


**Figure 13.** Temkin adsorption isotherm for the adsorption of MB dye onto AHC.

### Freundlich isotherm

The Freundlich equation is used to determinine the applicability of heterogeneous surface energy in the adsorption process [28]. The empirical Freundlich equation is expressed as:

$$\mathbf{\ln q_e = \ln K_F + \frac{1}{n} \ln C_e} \quad (7)$$

Where $k_f$ is a measure of adsorption capacity (mg $g^{-1}$) and n is adsorption intensity. 1/n values indicate the type of isotherm to be irreversible (1/n = 0), favourable (0<1/n<1), unfavourable (1/n >1). The plots of ln $q_e$ vs ln $C_e$ showed good linearity ($R^2$ = 0.98).The values of $K_f$ and n given in the Table 2. Values of n lies between 1 to 10 indicate an effective adsorption. It also indicates the degree of favorability of adsorption. The Freundlich adsorption capacity by this plot is 13.18 mg $g^{-1}$. Higher value of $k_f$ indicates higher affinity for MB adsorption. From these results it was clearly observed that both models were well suited for adsorption of MB on AHC, and the regression factor as

well as the calculated and experimental values are correlates correctly with both Langmuir and Freundlich isotherm.

**Temkin isotherm**

Temkin isotherm model predicts a uniform distribution of binding energies over the population of surface binding adsorption [28]. Linear form of Temkin equation is expressed as:

$$\mathbf{q_e = B\,lnA + B\,lnC_e} \quad (8)$$

Where B = RT/b, b is the Temkin constant related to heat of sorption $q_e$ (mg $g^{-1}$) and $C_e$ (mg $L^{-1}$) are the amount of adsorbed dye per unit weight of adsorbent and unabsorbed dye concentration in solution at equilibrium, respectively. Therefore, a plot of $q_e$ versus ln $C_e$ enables one to determine the constants A and B. From Table 2, AHC has maximum binding energy 2.99 J $g^{-1}$ which is uniformly distributed. The value for constant B is 10.26 J $mg^{-1}$ is heat of adsorption. High values of 'B' are observed in the steep initial slope of a sorption isotherm, indicating desirable high affinity. The correlation coefficient of 0.99 obtained showed that adsorption of MB also followed the Temkin model.

**3.11 Thermodynamic Study**

Thermodynamic studies were conducted at three different temperatures 300, 310 and 320 K. Parameters such as Free energy change ($\Delta G^\circ$), Enthalpy ($\Delta H^\circ$), and Entropy ($\Delta S^\circ$) which are used to decide whether the adsorption is a spontaneous process or not. Thermodynamic parameters can be calculated from the following equation.

$$\mathbf{\Delta G^o = -RT\,ln\,K_d} \quad (9)$$

Where R is the universal gas constant (8.314 $Jmol^{-1}\,K^{-1}$), T the temperature (K), and $K_d$ is the distribution coefficient. If the value of $\Delta G^\circ$ is negative, the chemical reaction can occur spontaneously at a given temperature. The $K_d$ value was calculated using the following Equation10.

$$\mathbf{K_d = \frac{C_e}{q_e}} \quad (10)$$

Where $q_e$ and $C_e$ are the equilibrium concentrations of MB (mg $L^{-1}$) on the adsorbent and in the solution, respectively. The enthalpy change ($\Delta H^\circ$) and entropy change ($\Delta S^\circ$) can be calculated from the following equation.

$$\mathbf{\Delta G^o = \Delta H^o - T\,\Delta S^o} \quad (11)$$

This equation can be written as

$$\mathbf{lnK_d = \frac{\Delta S^o}{R} - \frac{\Delta H^o}{RT}} \quad (12)$$

The thermodynamic parameters of $\Delta H^\circ$ and $\Delta S^\circ$ were obtained from the slope and intercept of the plot between log $K_d$ versus 1/T respectively from the Figure14.

The Gibbs free energy changes ($\Delta G^0$) were calculated from Equation 9, and the values of $\Delta G^\circ$, $\Delta H^\circ$, and $\Delta S^\circ$ for the adsorption of MB onto AHC were given in Table 3. The negative values of $\Delta G^0$ indicated the spontaneous nature of the adsorption process. The magnitude of $\Delta G^\circ$ also increased with increasing temperature indicating that the adsorption was more favorable at higher temperatures. The value of $\Delta H^0$ was positive indicating the endothermic nature of the adsorption of MB onto AHC. The adsorption of MB on the AHC was a

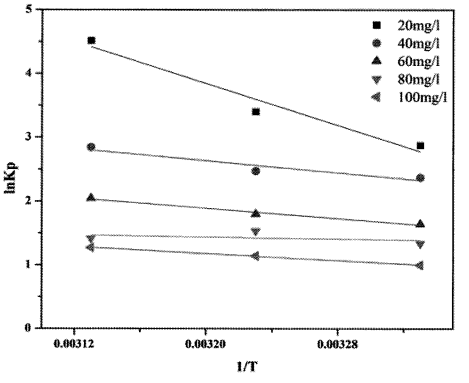


**Figure 14.** Vant-Hoff plot for the adsorption of MB dye onto AHC.

**Table 3.** Thermodynamic parameters for the adsorption of MB dye onto AHC.

| InitialConc (mg/l) | T (K) | $K_d$ | $\Delta G^\circ$ (J $mol^{-1}$) | $\Delta S^\circ$ (J $mol^{-1}$ $K^{-1}$) | $\Delta H^\circ$ (kJ $mol^{-1}$) |
|---|---|---|---|---|---|
| | 300 | 20.0 | -7171.9 | | |
| 20 | 310 | 30.5 | -8483.3 | 348.4 | 111.7 |
| | 320 | 62.0 | -11260.1 | | |
| | 300 | 7.9 | -5911.2 | | |
| 40 | 310 | 10.6 | -6163.0 | 279.8 | 89.9 |
| | 320 | 15.6 | -7094.4 | | |
| | 300 | 5.7 | -4092.5 | | |
| 60 | 310 | 6.8 | -4482.8 | 194.3 | 62.4 |
| | 320 | 8.3 | -5093.9 | | |
| | 300 | 4.1 | -3331.1 | | |
| 80 | 310 | 4.6 | -3822.3 | 156.1 | 50.2 |
| | 320 | 5.1 | -3519.3 | | |
| | 300 | 3.5 | -2487.6 | | |
| 100 | 310 | 4.1 | -2848.6 | 118.3 | 38.0 |
| | 320 | 4.9 | -3163.9 | | |

physical process because of the obtained $\Delta H^0$ value between +38 to +111.7 kJ $mol^{-1}$. Hence the adsorption equilibrium was rapidly attained and weak interactions between the MB and the functional groups on the surface of the adsorbent. Similar result obtained indigo onto silk yarn[29]. In addition, the positive value of $\Delta S^0$ suggested an increase in randomness at the solid/liquid interface during the adsorption of MB on the adsorbent.

### 3.12 Analysis of Variance

The results of analysis of variance (ANOVA) are given in Table 4. Statistical analysis of variance was performed to check whether the process parameters are statistically significant or not. The F-value for each process [30] indicates which parameter has a significant effect on the MB removal. Usually, the larger the F-value has the greater the effect on the MB removal. The influence of various parameters and their interaction on the removal percent was decided with the help of by ANOVA analysis and its performance characterized. The results of ANOVA for the removal of MB onto AHC are given in Table 4. Larger the F-value more is the effective parameter in the MB removal. The sequential order of the process variables is given below for MB removal onto AHC.

Temp>$C_o$ > PS> Carbon dosage>Time> pH

From the above order temp, initial concentration, dosage and particle size play a major role of adsorption of MB onto AHC but pH and time have a little impact when compare to the other parametric study.

## 4. CONCLUSIONS

Activated carbon prepared from areca husk carbon was effectively employed as an adsorbent for the removal of MB from aqueous solution. The surface morphology studies using SEM prove that, it contains more pores, that leads to develop more adsorption sites. The observed FTIR adsorbent spectral differences before and after adsorption indicated some of the peaks was disappearing due to the absorption of MB on AHC. Maximum adsorption of MB was found at pH 7, AHC dosage 150 mg, initial dye concentration of 10 mg $L^{-1}$ and an equilibrium time of 120 min. The maximum adsorption capacity of Areca husk carbon of methylene blue was found to be 46.3 mg $g^{-1}$. Value of $R_L$ was found to be 0.033 and confirmed that the prepared activated carbon is favourable for adsorption of MB dye. Kinetic data follow the

**Table 4.** ANOVA for various parameters for the adsorption of MB onto AHC.

| Parameter | DF | SS | MS | F Value | Prob>F |
|---|---|---|---|---|---|
| Dosage | 8 | 44852.43 | 14925.62 | 987.64 | 0.000000320 |
| Particle size | 7 | 44852.43 | 14945.16 | 3523.83 | 0.000000322 |
| Time | 16 | 89367.22 | 29772.89 | 7972.11 | 0.000000000 |
| Initial Concentration | 6 | 30218.52 | 10071.61 | 8167.99 | 0.000002488 |
| pH | 6 | 57560.76 | 19186.23 | 27678.92 | 0.000000040 |
| Temperature | 2 | 1.40081 | 1.34 | 23.45 | 0.004370000 |

***DF-Degree of freedom; SS-Sum of Squares; MS-Mean squares; F-Fischer.***

pseudo-first order kinetic model. Intra-particle diffusion model proves that pore diffusion plays major role in the dye adsorption. The calculated thermodynamic parameter shows the spontaneous and the endothermic nature of the adsorption process. ANOVA indicated that the most considerable factor was temp, concentration, particle size and adsorbent dosage. These results showed the possibility of AHC for MB dye removal from aqueous solution as an alternative to the costly used adsorbent employed in industries.

## ACKNOWLEDGEMENTS

The authors are grateful to Kumaraguru College of Technology for doing the research by providing some of the equipments for the research.

## REFERENCES

[1] Yi J.Z. and Zhang, L.M., *Bioresour. Technol.,* 2008; **99**: 2182-2186. DOI:10.1016/j.biortech.2007.05.028.

[2] Aygun A., Yenisoy-Karakas S. and Duman I., *Micropor. Mesopor. Mater.,* 2003; **66**: 189-195. DOI:10.1016/j.micromeso.2003.08.028.

[3] Weng C.H. and Pan Y.F., *Colloids Surfaces A: Physicochem. Eng. Aspect.,* 2006; **274**: 154-162. DOI:10.1016/j.colsurfa.2005.08.044.

[4] Batzias F.A., Sidiras D.K., Schroeder E. and Weber C., *Chem. Eng. J.,* 2009; **148**: 459-472. DOI:10.1016/j.cej.2008.09.025.

[5] Cengiz S. and Cavas L., *Bioresour. Technol.,* 2008; **99**: 2357-2363. DOI: 10.1016/j.biortech.2007.05.011.

[6] Wang, S., Boyjoo Y., Choueib A. and Zhu Z.H., *Water Res.,* 2005; **39**: 129-138. DOI:10.1016/j.watres.2004.09.011.

[7] Yavuz O. and Saka C., *Applied Clay Sci.,* 2013; **85:** 96-10. DOI:10.1016/j.clay.2013.09.011.

[8] Guo J.Z, Li B., Liu L. and Kangle L., *Chemosphere,* 2014; **111:** 225-231. DOI:10.1016/j.chemosphere.2014.03.118.

[9] Garg V.K., Amita M., Kumar R. and Gupta R., *Dyes Pigm.,* 2004; **63**: 243-250. DOI:10.1016/j.dyepig.2004.03.005.

[10] Bulut Y. and Aydin H.A., *Desalination,* 2006; **194**: 259-267. DOI:10.1016/j.desal.2005.10.032.

[11] Atef S. and Zaydien A.L., *Am. J. Environ.Sci.,* 2009; **5**: 197-208. DOI: 10.3844/ajessp.2009.197.208

[12] Janos P., Coskun S., Pilarova V. and Rejnek J., *Bioresour.Technol.,* 2009; **100:** 1450-1453. DOI: 10.1016/j.biortech.2008.06.069.

[13] Ahmed M.J. and Theydan S.K., *J.Anal. Appl. Pyrol.*, 2014; **105:** 199-208. DOI:10.1016/j.jaap.2013.11.005.

[14] Pavan F.A., Lima E.C., Dias S.L.P. and Mazzocato A.C., *J. Hazard. Mater.,* 2008; **150**: 703-712. DOI:10.1016/j.jhazmat.2007.05.023.

[15] Bestani B., Benderdouche N., Benstaali B., Belhakem M. and Addou A., *Bioresour. Technol.,* 2008; **99**: 8441-8444. DOI: 10.1016/j.biortech.2008.02.053.

[16] Pirbazari, A.E., Saberikhah E., Badrouh M. and Emami M.S., *Wat. Res. Ind.*, 2014; **6:** 64-80. DOI:10.1016/j.wri.2014.07.003.

[17] Ferrero F., *J. Hazard. Mater.,* 2007; **142:** 144-152. DOI:10.1016/j.jhazmat.2006.07.072.

[18] Kumar K.V. and Porkodi K., *J. Hazard. Mater.,* 2007; **146**: 214-226. DOI:10.1016/j.jhazmat.2006.12.010.

[19] Kushwaha A.K., Gupta N. and Chattopadhyaya M.C., *J.Saudi Chem. Soc.,* 2014; **18(3):** 200-207. DOI:10.1016/j.jscs.2011.06.011.

[20] Ofomaja A.E., *Desalination,* 2009; **3:** 1-10. DOI: 10.5004/dwt.2009.433

[21] Lata H., Garg V.K. and Gupta R.K., *Dyes Pigm.,* 2007; **74**: 653-658. DOI:10.1016/j.dyepig.2006.04.007.

[22] Vadivelan V. and Kumar K.V., *J. Colloid Interface Sci.,* 2005; **286**: 90-100. DOI:10.1016/j.jcis.2005.01.007.

[23] Banat F., Al-Asheh S., Al-Ahmad R. and Bni-Khalid F., *Bioresour. Technol.* 2007; **98**: 3017-3025. DOI:10.1016/j.biortech.2006.10.023

[24] Shabudeen P.S., Daniel S. and Indhumathi P., *Int. J. Res. Che. Environ.,* 2013; **3**: 60-65.

[25] McKay G. and Ho Y.S., *Process Biochem.,* 1999; **34**: 451-465. DOI: 10.1016/S0032-9592(98)00112-5.

[26] Webber W.J., *Principal and Application of Water Chemistry*, Wiley, New York, 1967.

[27] Ozcan A. and Ozcan A.S., *J. Hazard. Mater.,* 2005; **125**: 252-259. DOI:10.1016/j.jhazmat.2005.05.039

[28] Buasri A., Yongbut P., Chaiyut N. and Phattarasirichot K., *Chiang Mai J. Sci.* 2008; **35(1)**: 56-62.

[29] Kongkachuichay P., Shitangkoon A. and Hirunkitmonkon S., *Chiang Mai J. Sci.* 2010; **37(2):** 363-367.

[30] Ravikumar K., Ramalingam S., Krishnan S. and Balu K., *Dyes Pigm.,* 2006; **70**: 18-20. DOI:10.1016/j.dyepig.2005.02.004.